This is a repository copy of *Assessing variable amplitude multiaxial fatigue lifetime of notched components based on the notch critical plane approach*.

White Rose Research Online URL for this paper:
https://eprints.whiterose.ac.uk/166820/

Version: Accepted Version

Article:

Luo, P., Yao, W. and Susmel, L. orcid.org/0000-0001-7753-9176 (2020) Assessing variable amplitude multiaxial fatigue lifetime of notched components based on the notch critical plane approach. International Journal of Fatigue, 143. 105991. ISSN 0142-1123

https://doi.org/10.1016/j.ijfatigue.2020.105991

Article available under the terms of the CC-BY-NC-ND licence
(https://creativecommons.org/licenses/by-nc-nd/4.0/).

Reuse
This article is distributed under the terms of the Creative Commons Attribution-NonCommercial-NoDerivs (CC BY-NC-ND) licence. This licence only allows you to download this work and share it with others as long as you credit the authors, but you can’t change the article in any way or use it commercially. More information and the full terms of the licence here: https://creativecommons.org/licenses/

Takedown
If you consider content in White Rose Research Online to be in breach of UK law, please notify us by emailing eprints@whiterose.ac.uk including the URL of the record and the reason for the withdrawal request.

eprints@whiterose.ac.uk
https://eprints.whiterose.ac.uk/

Assessing variable amplitude multiaxial fatigue lifetime of notched components based on the notch critical plane approach

Peng Luo[1*], Weixing Yao[1,2], Luca Susmel[3]

[1]*State Key Laboratory of Mechanics and Control of Mechanical Structures, Nanjing University of Aeronautics and Astronautics, Nanjing 210016, China*

[2]*Key Laboratory of Fundamental Science for National Defense-Advanced Design Technology of Flight Vehicle, Nanjing University of Aeronautics and Astronautics, Nanjing 210016, China*

[3]*Department of Civil and Structural Engineering, the University of Sheffield, Sheffield S1 3JD, UK*

Abstract:

In the present paper, the notch critical plane method proposed by the authors is extended from 2D- to 3D-cases. The plane passing through the assumed critical point and experiencing the maximum variance of the resolved shear stress is defined as the the notch critical plane. The linear-elastic stress fields around the notch root are fitted via polynomial functions. The relationship between critical distance, l, and fatigue damage, D_b, under variable amplitude loading blocks is proposed. Susmel's parameter and a specific multiaxial cycle counting method are incorporrated into this approach to estimate multiaxial variable amplitude fatigue life. Numerous fatigue data generated by testing five different notched metallic materials were collected from the literature to check the accuracy of the proposed approach. This validation exercise allowed us to demonstrate that this method is highly accurate, with the majority of the predicted experimental results falling within an error band of 2.

Keywords: notched specimens; multixaial variable cyclic loading; maximum variance method

NOMENCLATURE

a,b	Material constant
A,B	Material constant
D	Fatigue damage
D_{cr}	The critical fatigue damage
E	Young's modulus
Δf_{-1}	The range of the fully reverse axial fatigue limit
G	Hessian matrix
ΔK_{th}	The range of the stress intensity factor threshold value
l_0	The critical distance in TCD
l	The critical distance in modified TCD
m	The index to consinder the effect of mean stress
N_f	the number of cycles to failure
r	The distance at notch root
σ_1	The maximum principal stress
σ_{-1}	The uniaxial endurance limit
σ_n	The maximum normal stress on critical plane
$\sigma_{n,m}$	The mean value of normal stress on critical plane.
$\sigma_{n,max}$	The maximum value of the normal stress on the critical plane
σ_x	The normal stress component
τ_{-1}	The torsional endurance limit
τ_a	The shear stress amplitude on the critical plane
$\varepsilon_f^{'}$	Fatigue ductility coefficient
$\Delta\varepsilon_n$	The amplitude of normal strain on critical plane

ABBREVIATION

AM	Area method
CA	Constant amplitude
FCP	Fatigue critical point
FEM	Finite element method
LEFM	Linear elastic fracture mechanics

LM	Line method
MVM	The maximum variance method
MVRSS	The maximum variance of resolved shear stress
NCP	Nocth critical plane
PM	Point method
SED	Strain energy density
SFI	Stress field intensity
TCD	The theory of critical distance
VA	Variable amplitude

1 Introduction

In industrial applications of practical interest, engineering structures and their components are subject to complex variable amplitude (VA) load histories which have high risk of causing fatigue failures [1–5]. Furthermore, fatigue cracks often initiate from notches, that is, from those regions experiencing localized stress/strain concentration phenomena. In this context, not only stress gradients, but also multiaxial stress states exist at the notch root even under uniaxial fatigue loading [6–9]. The effect of stress gradients, loading non-proportionality, stress multiaxiality, and profiles of the load spectra at the notch root should be taken into account to evaluate the fatigue lifetime of notched components under in-service VA load histories. The advanced volumetric approaches, such as the Strain Energy Density (SED) approach [10–12], the Stress Field Intensity approach (SFI) [13, 14] and the Theory of Critical Distances (TCD) [15] were proposed to assess the effect of stress gradients. In recent years, these approaches have been reviewed in detail in numerous technical articles – see, for instance, Refs [8, 16]. Among the above advanced volumetric approaches, the TCD is certainly the simplest one to be used in situations of practical interest. The TCD calculates the critical stress to be used to assess fatigue damage either at a point, along a line, over an area, or over a volume. The way the TCD works when used in the form of the Point Method (PM), Line Method (LM) and Area Method (AM) is schematically shown in **Figure 1**, with the different formalisations of this theory being formulated mathematically as follows:

$$
\begin{aligned}
&\text{Point Method(PM): } \sigma_{\text{av}} = \Delta\sigma_1\left(r=\frac{l_0}{2}, \theta=0\right) \\
&\text{Line Method(LM): } \sigma_{\text{av}} = \frac{1}{2l_0}\int_0^{2l_0} \Delta\sigma_1(r,\theta=0)\,dr \\
&\text{Area Method(AM): } \sigma_{\text{av}} = \frac{2}{1.1\pi l_0^2}\int_{-\pi/2}^{\pi/2}\int_0^{l_0} \Delta\sigma_1(r,\theta)\,r\,dr\,d\theta \\
&\text{Volume Method(VM): } \sigma_{\text{av}} = \frac{3}{2\pi(1.54l_0)^3}\int_0^{2\pi}\int_0^{\pi/2}\int_0^{1.54l_0} \Delta\sigma_1(r,\theta,\varphi)\,r^2\sin\theta\,dr\,d\theta\,d\varphi
\end{aligned}
\tag{1}
$$

$$\text{EL Haddad equation:} \quad l_0 = \frac{1}{\pi}\left(\frac{\Delta K_{\text{th}}}{\Delta f_{-1}}\right)^2 \tag{2}$$

In the above definitions, the critical distance, l_0, is defined via El Haddad's empirical equation [17] where Δf_{-1} and ΔK_{th} are the range of the uniaxial endurance limit and the range of the threshold value of the stress intensity factor (SIF), respectively.

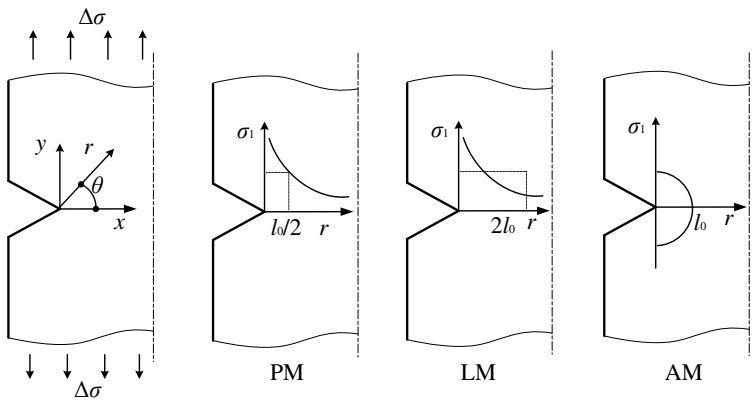

Figure 1. Visualisation of the Point Method, Line Method and Area Method.

Susmel and Taylor [2] have devised a novel method to estimate the fatigue lifetime of notched components under multiaxial VA cyclic loading based on their previous work. To assess fatigue damage, this approach makes use of Susmel's critical plane criterion [18–20] and the TCD PM. In this approach, the plane experiencing the maximum variance of the resolved shear stress (MVRSS) is regarded as the "critical plane". Then, the Three-Point Rain-Flow Cycle counting method is applied to count the cycles of the resolved shear stress. Besides, recently, Faruq and Susmel [3] further extended this design phylosophy by combing the modified Manson-Coffin curve method [21, 22] with the shear strain-maximum variance method [22, 23] and the elasto-plastic TCD [24, 25].

Similar to what was done by Susmel and co-workers, Gates and Fatemi [5, 26] recently have

proposed to combine the PM with a pseudo stress-based plasticity model to formulate an approach suitable for modelling the detrimental effect of local stress/strain gradients in the vicinity of notchs. In particular, Fatemi-Socie's equivalent parameter based on the critical-plane approach was applied to quantify damage under multiaxial VA fatigue loading. Having defined the plane experiencing the maximum fatigue damage as the critical plane, Wu *et al.* [27, 28] proposed to use a simple multiaxial cycle counting method based on Wu-Hu-Song (WHS) multiaxial parameter [29] to quantify fatigue lifetime under VA load histories. Hertel *et al.* [30] extended the short-crack model originally devised for multiaxial constant amplitude loading to multiaxial VA fatigue situations. In this approach, the plane with the maximum crack growth rate was defined as the critical plane. Tao *et al.* [31] combined the non-proportionality factor and Wang-Brown's multiaxial cycle counting approach [32–34] to predict multiaxial VA fatigue lifetime by calculating the elastic-plastic stress/strain fields around the notch tips.

In this paper, the notch critical plane approach (NCP) [9, 16] presented by the authors for the constant amplitude (CA) multiaxial fatigue case is initially extended from 2D- to 3D-situations and then applied to predict fatigue lifetime of notched components under complex VA fatigue loading. In this setting, the NCP is the plane experiencing the MVRSS and is taken coincident with that material plane passing through the assumed fatigue critical point (FCP) [7] - i.e. through the assumed crack initiation point at the notch root. Having defined the orientation of the NCP, the load history in terms of resolved shear stress amplitude and in terms of maximum normal stress on this plane are recorded. Then, the multiaxial cycle counting method proposed by the authors in Ref. [35] is used to count the fatigue cycles. Besides, the relation between critical distance, l, and fatigue damage, D_b, under multiaxial VA loading is proposed to modify the TCD. Over 120 experimental results generated by testing five different notched metallic materials were used to check the accuracy of the approach being proposed, with the majority predictions being

seen to fall within an error band of 2.

2 Determination of the NCP for 3D notches

2.1 NCP for notched specimens based on the MVM

In Refs [9] and [16], the notch critical plane at notch root was suggested to be defined as that material plane passing through the fatigue critical point and experiences the maximum amplitude of the shear stress. The NCP is based on the assumption that the initiation of micro-cracks is driven by the shear stress. By testing under CA multiaxial fatigue loading a large number of specimens made of 2297 lithium-aluminium alloy, Luo *et al.* [16] demonstrated that the orientation of the NCP is the same as the orientation of the crack initiation at the notch root. Further, the NCP was seen to be sucesfull in estimating the multiaxial CA fatigue lifetime of notched components, with different critical-plane multiaxial fatigue criteria, such as Susmel's criterion or ZY's parameter [36], being used to quantify the fatigue life.

The NCP was originally proposed for 2D-notched components under multiaxial CA cyclic loading. In the present study, the NCP is extended from 2D- to 3D-cases to assess fatigue damage in notched components under multiaxial VA cyclic loading based on the maximum variance method (MVM). The MVM can easily determine the orientation of the critical plane by using the standard optimization algorithms that are available in different commercial codes, for instance, Matlab®. The traditional approach to determine the orientation of the critical plane is to calculate the shear stress amplitude or other mechanical quantities on a large number of different planes. Unfortunately, this *modus operandi* is very time-consuming, especially in the presence of 3D components. The MVM is can be applied along with standard optimization algorithms and the critical plane is defined as the plane experiencing the MVRSS [23, 35].

To simplify the process of determing the NCP in the vicinity of notches, the plane passing

through the FCP and experiencing the MVRSS is regarded as the NCP. The first step to locate the orientation of the NCP is to determine the FCP which is nothing but the crack initiation point, where, usually, cracks initiate from the surface of the notched components being designed. Analytical solutions around the notches can be obtained for standard notches, such as circle holes or V-notchs. In contrast, the numerical solutions around non-standard notches can be obtained by the FEM.

The idea to determine the FCP is to estimate the fatigue damage of the whole potential points around the notch, then the point exoeriecing the maximum value of the fatigue damage is defined as the FCP. The details to locate the FCP were introduced in Ref. [7] where a large number of notched specimens made of of 2297 luminium-lithium alloy and GH4169 nickel-base superalloy were tested under multiaxial fatigue loading to verify the accuracy of FCP around the notches being investigated. In this context, it should be noticed that suitable cycle counting methods had to be used to estimate lifetime under multiaxial VA fatigue loading.

A notched specimen under multiaxial VA fatigue loading is shown in **Figure 2** where the point O is the FCP. Point O is regarded as the origin in **Figure 3**(*a*), where O-*xyz* is the global system of coordinates and O-*abn* is the local system of coordinates. Besides, O-$r\phi\theta$ is the spherical system of coordinates referring to O-*abn*. $\boldsymbol{n}$ is the normal vector of plane △. Vector $\boldsymbol{r}$ is the vector $\boldsymbol{n}$ in the local spherical coordinate O-$r\phi\theta$. The resolved shear stress, τ_q(t), on the plane △ is the projection of the shear stress τ_n(t) along a direction which is at angle α to axis a. Unit vectors $\boldsymbol{n}$ and $\boldsymbol{q}$ are expressed as follows:

$$\boldsymbol{n}=\begin{bmatrix} n_x \\ n_y \\ n_z \end{bmatrix}=\begin{bmatrix} \sin\theta\cos\phi \\ \sin\theta\sin\phi \\ \cos\theta \end{bmatrix} \qquad \boldsymbol{q}=\begin{bmatrix} q_x \\ q_y \\ q_z \end{bmatrix}=\begin{bmatrix} \cos\alpha\sin\phi+\sin\alpha\cos\theta\cos\phi \\ -\cos\alpha\cos\phi+\sin\alpha\cos\theta\sin\phi \\ -\sin\alpha\sin\theta \end{bmatrix} \tag{3}$$

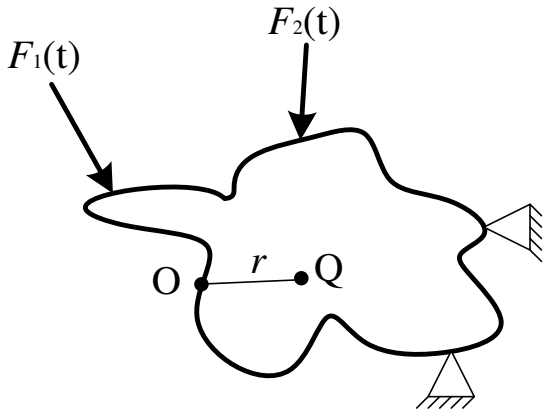

Figure 2. The notched specimen under multiaxial VA fatigue loading.

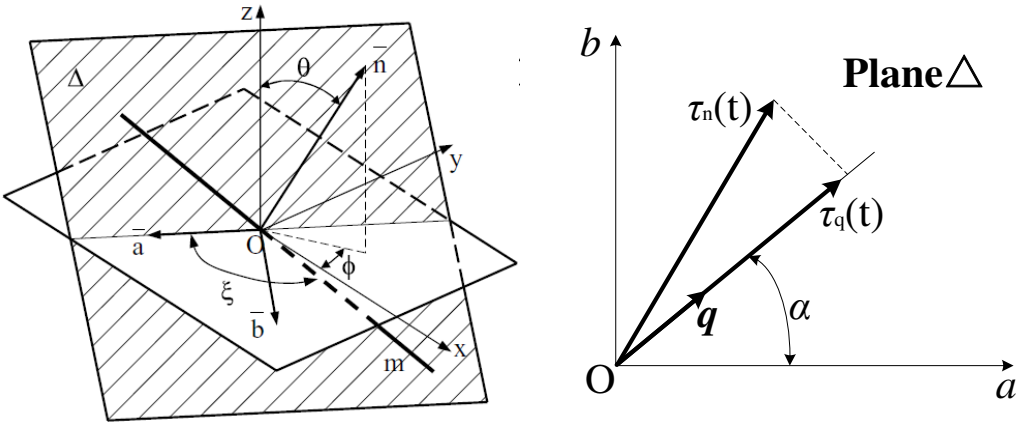

(*a*) (*b*)

Figure 3. The illustration of the local spherical coordinate O- $r\phi\theta$ and the resolved shear stress.

The resolved shear stress $\tau_q(t)$ is determined as:

$$\tau_q(t) = \boldsymbol{q}^T \cdot \boldsymbol{\sigma}_{ij}(r,\phi,\theta,t) \cdot \boldsymbol{n} = \begin{bmatrix} q_x & q_y & q_z \end{bmatrix} \begin{bmatrix} \sigma_x & \tau_{xy} & \tau_{xz} \\ \tau_{xy} & \sigma_y & \tau_{yz} \\ \tau_{xz} & \tau_{yz} & \sigma_z \end{bmatrix} \begin{bmatrix} n_x \\ n_y \\ n_z \end{bmatrix} = \boldsymbol{D} \cdot \boldsymbol{s}(r,\phi,\theta,t) \tag{4}$$

where $\boldsymbol{\sigma}_{ij}$ is the local stress tensor field around the FCP.

$$\boldsymbol{D}=\begin{bmatrix} D_1 \\ D_2 \\ D_3 \\ D_4 \\ D_5 \\ D_6 \end{bmatrix}^{\mathrm{T}}=\begin{bmatrix} n_x q_x \\ n_y q_y \\ n_z q_z \\ n_x q_y + n_y q_x \\ n_x q_z + n_z q_x \\ n_y q_z + n_z q_y \end{bmatrix}^{\mathrm{T}}=\begin{bmatrix} \frac{1}{2}\left(\sin\theta\sin 2\phi\cos\alpha+\sin\alpha\sin 2\theta\cos^2\phi\right) \\ \frac{1}{2}\left(-\sin\theta\sin 2\phi\cos\alpha+\sin\alpha\sin 2\theta\sin^2\phi\right) \\ -\frac{1}{2}\sin\alpha\sin 2\theta \\ \frac{1}{2}\sin\alpha\sin 2\phi\sin 2\theta-\cos\alpha\cos 2\phi\sin\theta \\ \sin\alpha\cos\phi\cos 2\theta+\cos\alpha\sin\phi\cos\theta \\ \sin\alpha\sin\phi\cos 2\theta-\cos\alpha\cos\phi\cos\theta \end{bmatrix}^{\mathrm{T}} \tag{5}$$

$$\boldsymbol{s}(t)=\begin{bmatrix} s_1 \\ s_2 \\ s_3 \\ s_4 \\ s_5 \\ s_6 \end{bmatrix}=\begin{bmatrix} \sigma_x(r,\phi,\theta,t) \\ \sigma_y(r,\phi,\theta,t) \\ \sigma_z(r,\phi,\theta,t) \\ \sigma_{xy}(r,\phi,\theta,t) \\ \sigma_{xz}(r,\phi,\theta,t) \\ \sigma_{yz}(r,\phi,\theta,t) \end{bmatrix} \tag{6}$$

The variance of the resolved shear stress is:

$$\begin{aligned} \mathrm{Var}\left[\tau_{\mathrm{q}}(t)\right] &= \mathrm{Var}\left[\boldsymbol{D}\cdot\boldsymbol{s}(t)\right]=\mathrm{Var}\left[\sum_{k=1}^{6}\left(D_k\cdot s_k\right)\right] \\ &=\sum_{k=1}^{6}\left\{D_k^2\cdot\mathrm{Var}\left[s_k\right]\right\}=\boldsymbol{D}\cdot\mathrm{Var}\left[\boldsymbol{s}\right]\cdot\boldsymbol{D}^{\mathrm{T}} \\ &=\boldsymbol{D}\cdot\boldsymbol{C}(r,\phi,\theta)\cdot\boldsymbol{D}^{\mathrm{T}} \end{aligned} \tag{7}$$

where,

$$\boldsymbol{C}=\begin{bmatrix} V_x & C_{x,y} & C_{x,z} & C_{x,xy} & C_{x,xz} & C_{x,yz} \\ C_{x,y} & V_y & C_{y,z} & C_{y,xy} & C_{y,xz} & C_{y,yz} \\ C_{x,z} & C_{y,z} & V_z & C_{z,xy} & C_{z,xz} & C_{z,yz} \\ C_{x,xy} & C_{y,xy} & C_{z,xy} & V_{xy} & C_{xy,xz} & C_{xy,yz} \\ C_{x,xz} & C_{y,xz} & C_{z,xz} & C_{xy,xz} & V_{xz} & C_{xz,yz} \\ C_{x,yz} & C_{y,yz} & C_{z,yz} & C_{xy,yz} & C_{xz,yz} & V_{yz} \end{bmatrix} \tag{8}$$

$$V_i=\frac{1}{T}\int_0^T\left[\sigma_i(r,\phi,\theta,t)-E(\sigma_i)\right]^2dt=V_i(r,\phi,\theta) \tag{9}$$

$$C_{i,j}=\frac{1}{T}\int_0^T\left\{\left[\sigma_i(r,\phi,\theta,t)-E(\sigma_i)\right]\cdot\left[\sigma_j(r,\phi,\theta,t)-E(\sigma_j)\right]\right\}dt=C_{i,j}(r,\phi,\theta) \tag{10}$$

$$E(\sigma_i)=\frac{1}{T}\int_0^T\sigma_i(r,\phi,\theta,t)dt \tag{11}$$

Matrix $\boldsymbol{C}$ in Eq.(7) depends on the orientation of plane △ and the distance, r, between the FCP and the selected point Q (see **Figure 2**) at the notched root. However, matrix $\boldsymbol{C}$ for plain specimens is a constant matrix only depending on the loading history because of the uniform

stress field [35].

The distance, *r,* gives a measurement of how large the fatigue damage area is at the notch root. In the authors' opinion, the fatigue damage area is nothing but the process zone whose size depends on both material morphology and characteristics of the damaging process taking place. In this context, continuum mechanics is not suitable to model the crack initiation phase because the assumption of continuous and homogenous material is no longer valid. The local stress and the local micro-structure deeply influence the direction of crack initiation. Besides, a conclusion has been drawn in the authors' recent research that the maximum length of crack initiation is the critical distance l_0 of TCD [16].

According to the above analysis that the maximum length of crack initiation is l_0 so that Eq.(2) is introduced into Eq.(7) as follows:

$$f(\phi,\theta,\alpha)=\mathrm{Var}\left[\tau_{\mathrm{q}}(t)\right]=\boldsymbol{D}\cdot\boldsymbol{C}(l_0,\phi,\theta)\cdot\boldsymbol{D}^{\mathrm{T}} \tag{12}$$

The plane passing through the FCP and experiencing the MVRSS is defined as the NCP in the presence of notches. Therefore, the orientation of the NCP is given by the angle $(\phi_{\mathrm{m}},\theta_{\mathrm{m}})$ which results in the maximum value for $\mathrm{Var}\left[\tau_{\mathrm{q}}(t)\right]$. The gradient optimization algorithm can be used to find the maximum of Eq. (12). Two classical gradient optimization algorithms, i.e., the Conjugate Gradient Method and Newton's method, were used by the authors in Ref. [35] to find, in the absemce of gradient, the critical plane experiencing the MVRSS. Newton's method is taken as an example to show how the gradient optimization algorithm is used to find the maximum of Eq. (12). The flow chart of the searching process by using the Newton method is shown instead in **Figure 4**.

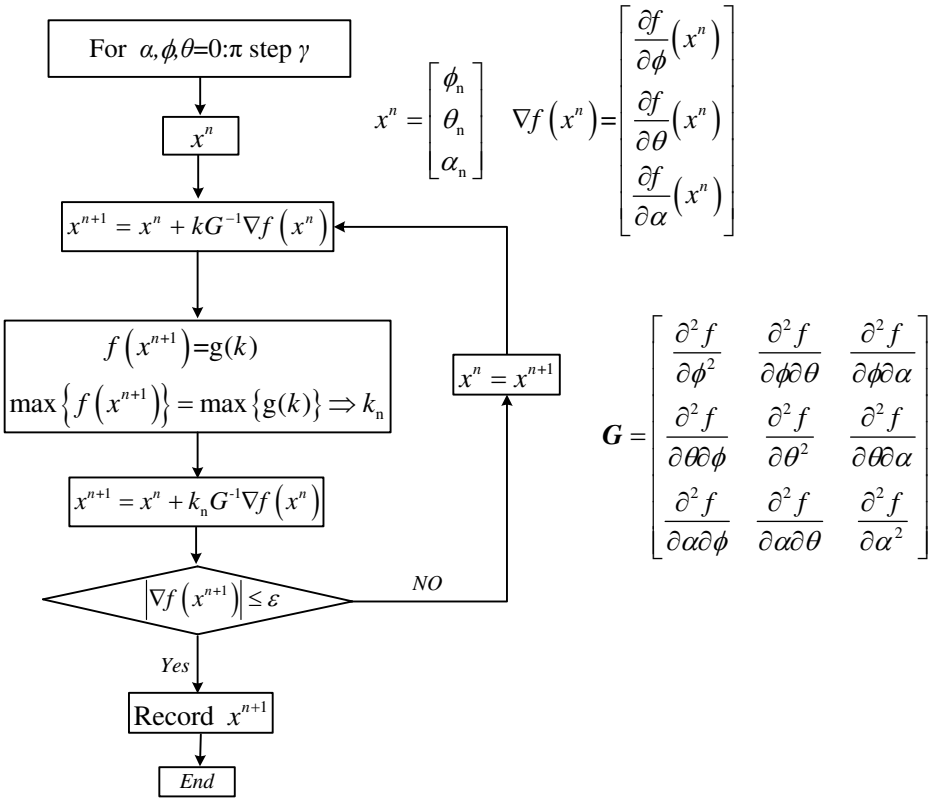

Figure 4. the illustration of the Newton method to search NCP for notched specimens.

It should be noticed that the difference between plain and notched materials when it comes to searching for the critical plane via gradient optimization algorithm lies in matrix ***C***. In the absece of notches, Matrix ***C*** can be regarded as a constant matrix during the iterative solution and it only depends on the stress tensor history. In contrast, the matrix ***C*** needs to be updated for each iterative step for notched specimens because it not only depends on the local stress tensor history, but also on the orientation of the selected plane. Therefore, the calculation process to determine the critical plane of notched components is more complex than that required for smooth components.

2.2 Approximate analytical solutions for the local elastic stress fileds at the notch tip

As mentioned above, in Eq. (4) $s(r,\phi,\theta,t)$ are the analytical solutions for the local elastic

stress fileds at the notch root. However, it is very diffcult to solve the analytical solutions $s(r,\phi,\theta,t)$ around the notch root especially under multiaxial fatigue loading. Although the numerical stress fileds around the notch can be calculated by the finite element method (FEM), these solutions are the stress states of discrete nodes around the notch root. The solutions of FEM are not convenient for the iterations shown in **Figure 4**.

A simple method to get the approximate analytical solutions of local elastic stress fileds at the notch root is introduced based on linear elasticity and the superposition principle. This method can also reduce the computational time especially in the presence of VA load histories.

The way the superposition principle is employed is shown in **Figure 5**. In particular, two functions $f_{1A}(x,y,z)$ and $f_{2A}(x,y,z)$ are used to fit the discrete stress fields calculated by the FEM around the point A under unit forces F_1 and F_2, respectively.

According to linear elasticity and the superposition principle, the fitted stress field around point A under $n_1F_1+ n_2F_2$ is:

$$\sigma_A(x,y,z)=n_1F_1f_{1A}(x,y,z)+n_2F_2f_{2A}(x,y,z) \tag{13}$$

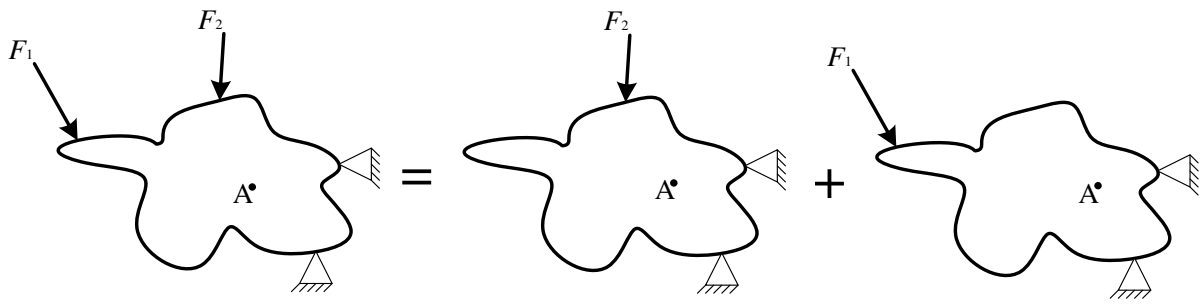

Figure 5. the illustration of superposition principle.

The fitted functions of the local stress field have many different forms, which are based on the notch type. However, independently of the notch type, polynomial function can always be used to fit the stress filed around the notch. A fitted function is suggested as follows:

$$\sigma_{ij}(r,\theta,\phi)=\left(\sum a_i r^i\right)\cdot\left[\sin\left(\sum b_i\theta^i\right)\right]\cdot\left[\cos\left(\sum c_i\phi^i\right)\right] \tag{14}$$

The parameters in Eq.(14) can easily be solved by using the Least Squares Method as implemented, for instance, in Matlab. It is worth noting that Eq.(14) is only the approximate analytical solution for the local elastic stress fileds around the notches under investigation. The fitting precision depends on the number of parameters in Eq.(14). Fifteen parameters (three variables r, θ and ϕ up to the fourth power) are enough to accurately fit the elastic stress fields at the notch root.

The notched specimen under tension-torsional VA loading shown in **Figure 6** is taken as an example to explain how Eq. (13) works. The elastic stress fields around the notch root under force F_0 and T_0 are $\sigma_{F_0 ij}(r,\theta,\phi)$ and $\sigma_{T_0 ij}(r,\theta,\phi)$ respectively. According to linear elasticity and the superposition principle, the stress field around the notch root under both the force $F(t)$ and force $T(t)$ at time t is:

$$\sigma_{ij}(r,\theta,\phi,t) = \frac{F(t)}{F_0}\sigma_{F_0 ij}(r,\theta,\phi) + \frac{T(t)}{T_0}\sigma_{T_0 ij}(r,\theta,\phi) \tag{15}$$

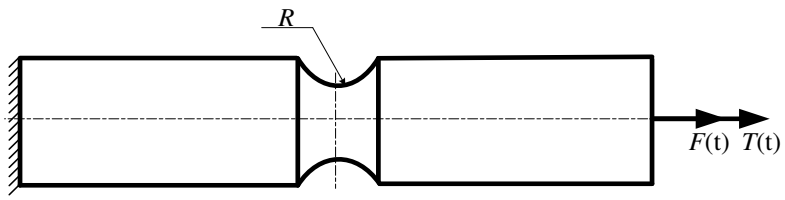

Figure 6. Notched specimens under tension-torsional VA loading.

It is simple and effective to obtain the elastic stress field around the notch root at any time under VA loading because only several basic elastic stress fields around the notch root need to be analyzed using the FEM and fitted functions.

3 The relation between critical distance and fatigue damage

Based on Linear Elastic Fracture Mechanics (LEFM), the TCD was initially proposed to predict fatigue damage in the high-cycle fatigue regime [15]. Susmel *et al.* [37] extended the use

of the TCD from the high-cycle fatigue to the medium/low-cycle fatigue regime by assuming that a power function exists between the critical distance, *l,* and the number of cycles to failure, N_f, i.e.:

$$l = a\left(N_f\right)^b \tag{16}$$

where, *a* and *b* are two material parameters to be determined experimentally. In particular, parameters *a* and *b* can be determined by two *S-N* curves separately. One is the *S-N* curve from the plain specimens and the other is the *S-N* curve from specimens containing a known geometrical feature [37]. The *S-N* curve of the plain specimens can be obtained by conducting fatigue tests under simple uniaxial loading.

The 'stress-distance' curve at the notch root is assumed to be like the one seen in **Figure 7** and the fatigue lifetimes of two notched specimens under different fatigue loadings are assumed to be N_1 and N_2, respectively. The *S-N* curve of the plain specimens is:

$$S = A\left(N_f\right)^B \tag{17}$$

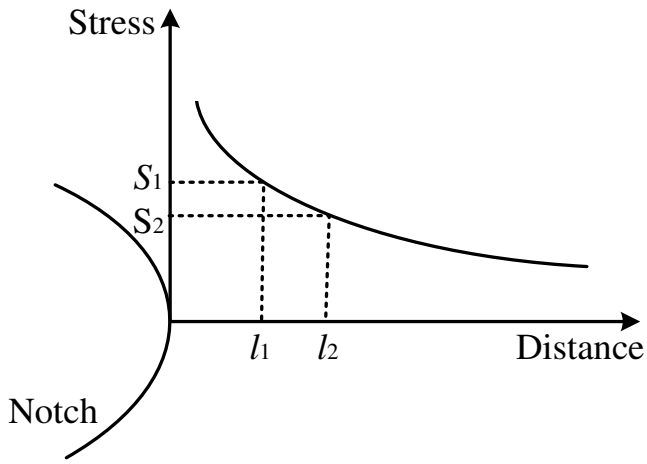

Figure 7. 'Stress-distance' curve at the notch root.

It should be noticed that stress S_1 and S_2 corresponding to N_1 and N_2, respectively, can be calculated from the *S-N* curve in Eq.(17). l_1 and l_2 are the effective critical distance values for

two notched specimens with different fatigue life in **Figure 7**. The parameters a and b in Eq.(14) can be derived as follows:

$$b = \frac{\lg l_1 - \lg l_2}{\lg N_1 - \lg N_2}$$
$$a = \frac{l_1}{(N_1)^{\frac{\lg l_1 - \lg l_2}{\lg N_1 - \lg N_2}}} \tag{18}$$

Moving to VA situations, the number of loading blocks N_b represents the fatigue life under a given VA load history. Besides, under CA fatigue loading, the high-cycle fatigue regime and the low-cycle fatigue regime can be distinguished via the number of cycles. In contast, they can not be distinguished via the number of cycles under VA fatigue loading. Thus, Eq.(16) can not be applied for VA loading because the length and magnitude of different VA loadings are not unified. According to Miner's rule, fatigue damage can be quantified as:

$$D=\frac{D_{cr}}{N_f} \ or \ D=\frac{D_{cr}}{N_b} \tag{19}$$

where, N_f and N_b are the cycles to fatigue failure under constant amplitude and VA loading respectively. D_{cr} is the critical value of the damage sum.

Eq. (19) is introduced into Eq. (16) as follows:

$$l=a\left(\frac{D_{cr}}{D}\right)^b \tag{20}$$

In the above equation, D is equal to the critical fatigue damage, D_{cr}, when the fatigue block under VA loading is one. Eq. (20) can be applied for VA loading and the length of l depends on the fatigue damage of one loading block.

The process to estimate the fatigue lifetime of notched specimens under multiaxial VA loading is shown in **Figure 8**. Susmel's parameter [18–20], one of the multiaxial damage parameters based on the critical plane approach, is applied to assess fatigue damage. The plane experiencing the maximum amplitude of the shear stress is taken as the critical plane [18–20]. Susmel's criterion can be formulated as:

$$\tau_{\mathrm{eq}} = \tau_a + \left(\tau_{-1} - \sigma_{-1}/2\right)\left[\min\left(\rho_0, \rho_{\mathrm{lim}}\right)\right] \tag{21}$$

$$\rho_0 = \frac{\sigma_{\mathrm{n,max}}}{\tau_a} = \frac{\sigma_{\mathrm{n},a} + m\sigma_{\mathrm{n},m}}{\tau_a} \tag{22}$$

$$\rho_{\mathrm{lim}} = \frac{\tau_{-1}}{2\tau_{-1} - \sigma_{-1}} \tag{23}$$

where σ_{-1} and τ_{-1} are the uniaxial endurance limit and the torsional endurance limit, respectively. m is the index suitable for consindering the effect of mean stress and m can be obtained by running *ad hoc* tests. τ_{a} is the shear stress amplitude and $\sigma_{\mathrm{n,max}}$ is the maximum value of the normal stress on the critical plane.

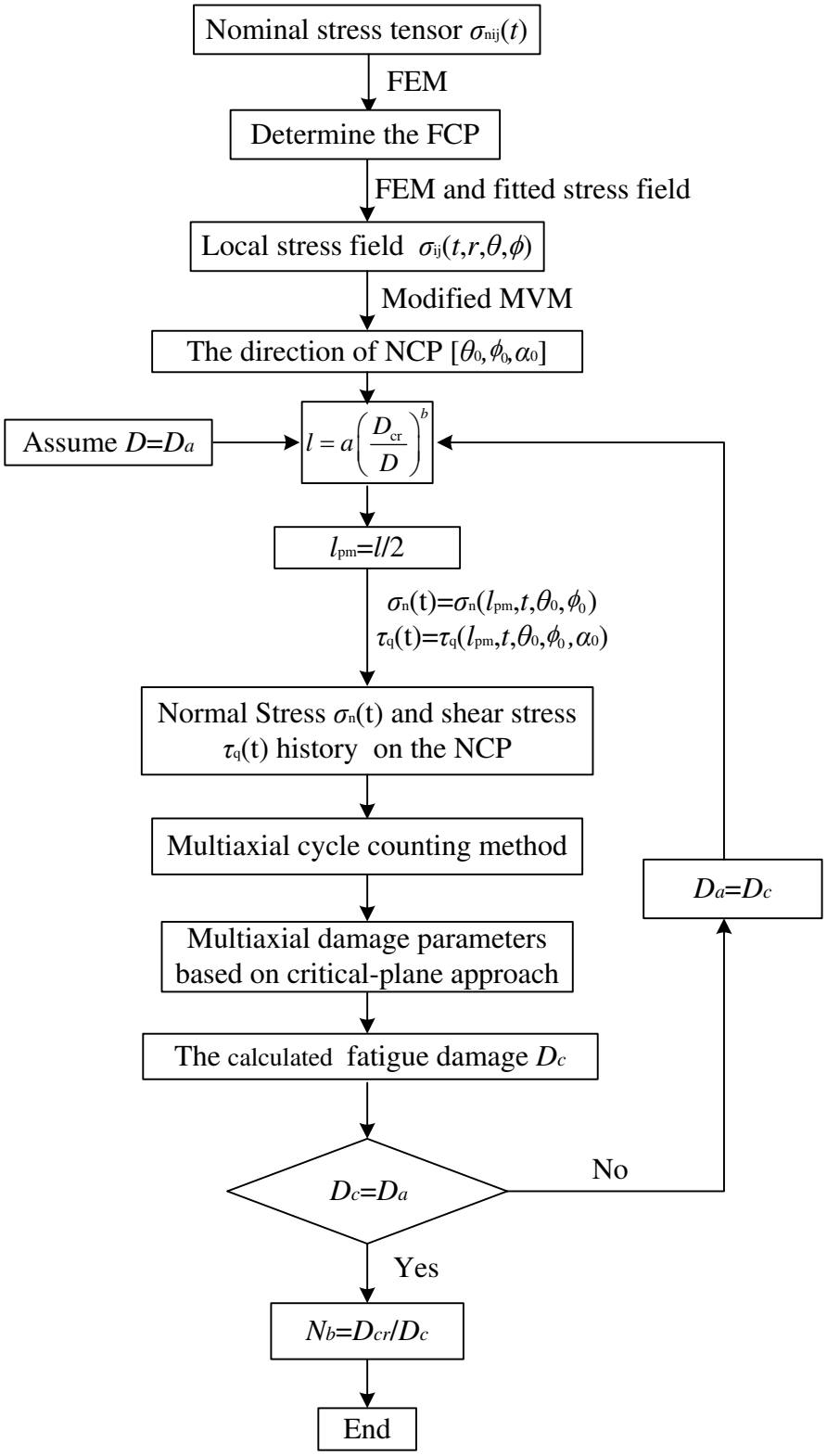

Figure 8. the process to estimate the fatigue life of notched components under multiaxial VA loading.

It should be noticed that there are several approaches suitable for counting fatigue cycles under multiaxial VA loading, such as, Bannantine-Socie's method [38], Wang-Brown's solution [32–34] and Carpinteri's approach [39]. The multiaxial cycle counting method recently proposed by the authors [35] is used in what follows to verify the robustness and accuracy of the methodology summarized in Figure 8. The one-dimensional resolved shear stress on the NCP is taken as the first channel and the normal stress on the NCP is taken as the second channel in the multiaxial cycle counting method. The first channel, i.e., resolved shear stress τ_q, is counted by using the Rain-Flow Cycle Counting Method and the maximum and the minimum of the normal stress within the cycle of τ_q are recorded to obtain the mean and the amplitude of the normal stress on the notch critical plane. The way this multiaxial cycle counting method works is illustrated in **Figure 9** where the resolved shear stress amplitude $\triangle\tau_a$ between time 1 and 5 is counted by the Rain-Flow Cycle Counting Method and the maximum and the minimum normal stress between time 1 and 5 are $\sigma_{n,max}$ and $\sigma_{n,min}$ respectively.

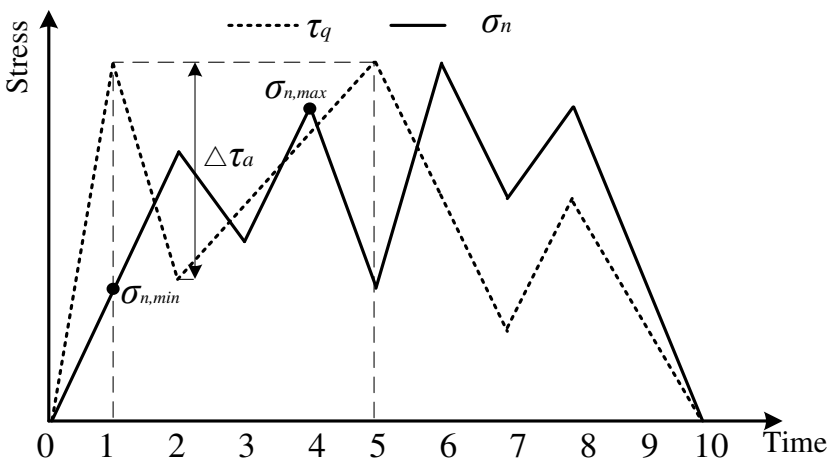

Figure 9. the illustration of the multiaxial cycle counting method [35].

4 Evaluation and Validation

4.1 Test data collected

Multiaxial VA fatigue data generated by testing five different metallic materials (C40 [2], TC4 [40], En8 [3], S460N [30, 41], 2024-T3 [4, 5, 26]) were gathered from the published literature and used to verify the accuracy of the design approach being proposed. The mechanical and fatigue properties of the considered materials are summarized in **Table 1**. Dimensions and the FE models of the notched specimens being investigated are shown in Appendix 1.

Table 1. The mechanical property parameters

Materials	E/GPa	σ_b/MPa	σ_{-1}/MPa	τ_{-1}/MPa
C40	209	850	292.8	231.7
TC4	108.4	945.2	248.3	192.4
En8	210	701	223.3	179.6
S460N	208.5	643	243	220
2024-T3	73.7	495	168	120

4.2 Analysis of collected fatigue test

The multiaxial VA fatigue damage associated with the collected notch results was estimated according to the procedure shown in Figure 8. It should be noticed that the linear-elastic FE models were used to analyze the local stress fields around the notch roots by using software Patran 2012. Miner's linear cumulative damage rule was used to estimate VA fatigue damage. Although it is equal to one in Miner's rule, the critical damage, D_{cr}, is always difficult to quantify accurately. In fact, D_{cr} usually ranges from 0.02 to 5 and the only way to determine it is by running specific experiments. On the basis of a large number of tests, Sonsino *et al*. [42–44] proposed that D_{cr} should be taken equal to 0.37 for aluminum and to 0.27 for the steel to always reach the wanted level of safety for the component being designed. The predicted fatigue lifetimes of the considered notched samples are listed in **Figure 10**. The majority of the predicted numbers of cycles to failure falls within an error band of 2, with all the estimates falling into error band of 4. The error of prediction is mainly due to the limitations associated with the

linear-elastic stress field around the notch root. The accuracy can be improved if elastic-plastic FEM analyses are introduced. However, it is time-consuming to analyze the elastic-plastic stress fields around notch roots especially for 3D notched components. The predicted lifetime is acceptable and the process is quick and simple based on linear-elastic FEM.

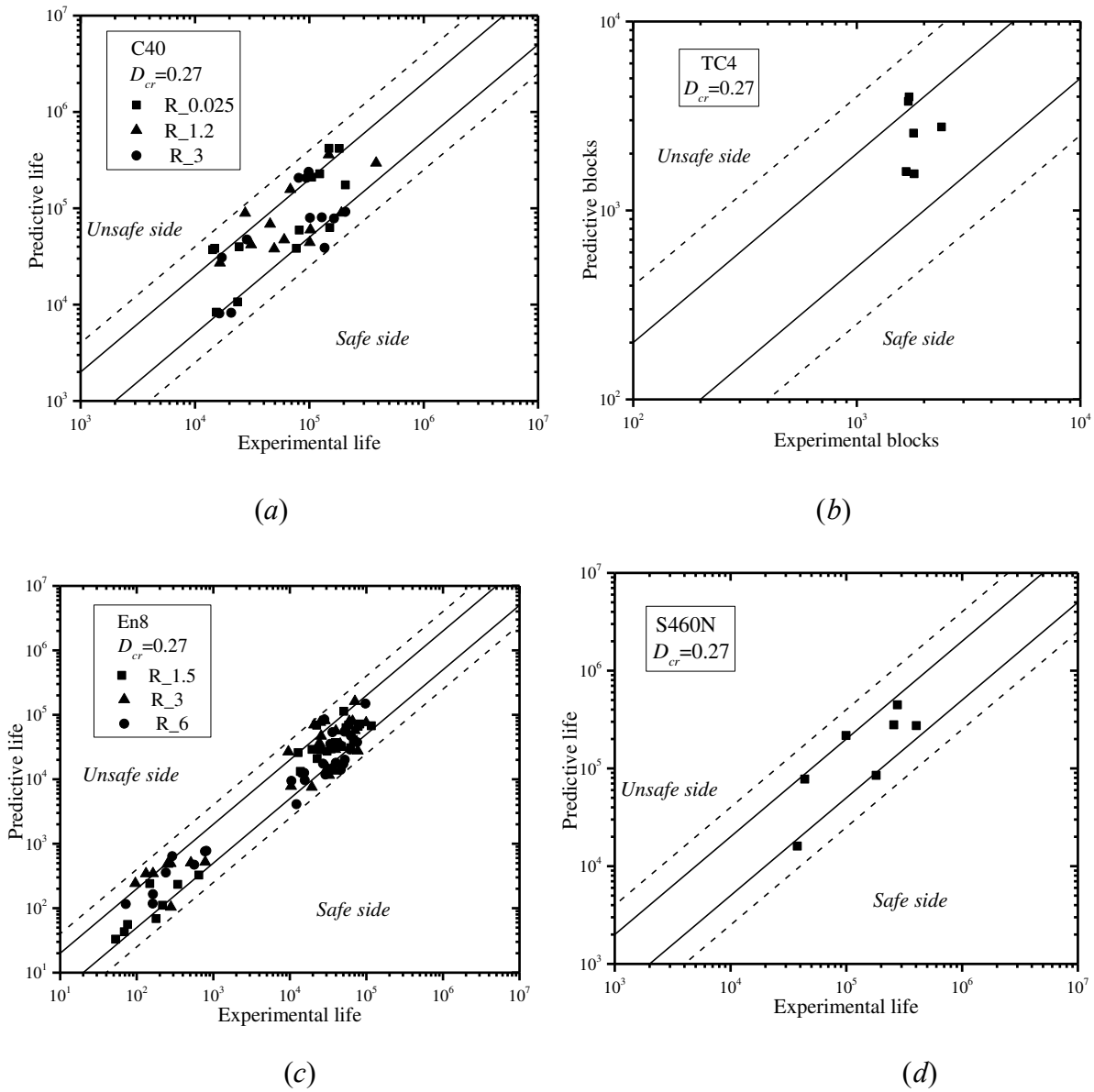

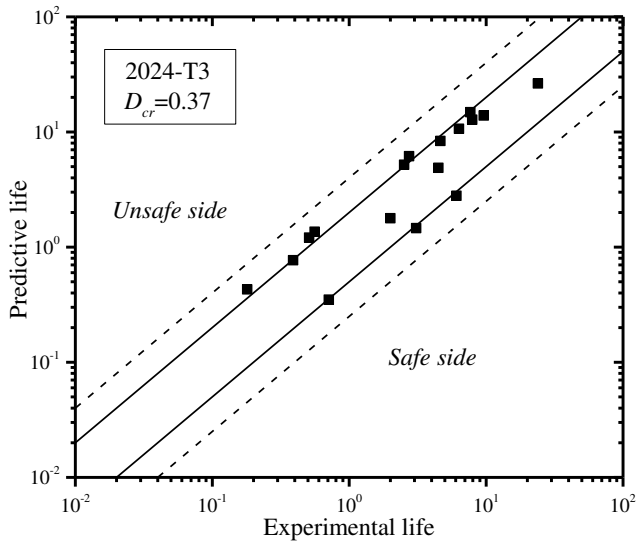

(*e*)

Figure 10. Predicted multiaxial VA fatigue life for the nocthed specimens being considered.

5 Conclusion

(1) The NCP method is extended from 2D to 3D-situations based on the MVM. The plane passing through the FCP and experiencing the MVRSS is defined as the notch critical plane.

(2) The relevant elastic stress fields are obtained based on linear elasticity and the superposition principle. Polynomial function are used to fit the elastic stress fields at the notch root and only linear-elastic FEM is needed for notched specimens.

(3) The relation between critical distance l and fatigue damage D_b is applied to estimate VA fatigue damage by combing Susmel's parameter and the multiaxial cycle counting method recently raised by the authors.

(4) Multiaxial VA fatigue test data from five notched metallic materials were collected to check the accuracy of the proposed approach. The majority of the predicted lifetime was seen to fall within error band of 2 and the error is mainly due to the assumption of linear-elastic stress fields around the notch root.

6 Acknowledgement

The authors acknowledge the support from China Scholarship Council (CSC201906830050) and National Science and Technology Major Project (2017-Ⅵ-0003-0073).

7 References

[1] Susmel L, Tovo R, Benasciutti D. A novel engineering method based on the critical plane concept to estimate the lifetime of weldments subjected to variable amplitude multiaxial fatigue loading. *Fatigue Fract Eng Mater Struct*. 2009; 32(5): 441–459.

[2] Susmel L, D. Taylor. A critical distance/plane method to estimate finite life of notched components under variable amplitude uniaxial/multiaxial fatigue loading. *Int J Fatigue*. 2012;38(5):7–24.

[3] Faruq NZ, Susmel L. Proportional/nonproportional constant/variable amplitude multiaxial notch fatigue: cyclic plasticity, non-zero mean stresses, and critical distance/plane. *Fatigue Fract Eng Mater Struct*. 2019;42(9):1849–1873.

[4] Gates NR, Fatemi A. Multiaxial variable amplitude fatigue life analysis using the critical plane approach, Part I: Un-notched specimen experiments and life estimations. *Int J Fatigue*. 2017;105(12):283–295.

[5] Gates NR, Fatemi A. Multiaxial variable amplitude fatigue life analysis using the critical plane approach, Part II: Notched specimen experiments and life estimations. *Int J Fatigue*. 2018;106(1):56–69.

[6] Susmel L. The theory of critical distances: a review of its applications in fatigue. *Eng Fract Mech*. 2008;75(7):1706–1724.

[7] Luo P, Yao WX, Susmel L, Li P. Prediction methods of fatigue critical point for notched components under multiaxial fatigue loading. *Fatigue Fract Eng Mater Struct*. vol. 2019;42(12):2782–2793.

[8] Luo P, Yao WX, Wang YY, Li P. A survey on fatigue life analysis approaches for metallic notched components under multi-axial loading. *Proceedings of the Institution of Mechanical Engineers, Part G: Journal of Aerospace Engineering*. 2019; 233(10):3870–3890.

[9] Luo P, Yao WX, Li P. A notch critical plane approach of multiaxial fatigue life prediction for metallic notched specimens. *Fatigue Fract Eng Mater Struct*. 2019; 42(4):854–870.

[10] Lazzarin P, Zambardi R. A finite-volume-energy based approach to predict the static and fatigue behavior of components with sharp V-shaped notches. *Int J Fract*. 2001;112(3):275–298.

[11] Lazzarin P, Tovo R. A notch intensity factor approach to the stress analysis of welds. *Fatigue*

Fract Eng Mater Struct. 1998;21(9):1089–1103.

[12]Lazzarin P, Lassen T, Livieri P. A notch stress intensity approach applied to fatigue life predictions of welded joints with different local toe geometry', *Fatigue Fract Eng Mater Struct*. 2003;26(1):49–58.

[13]Gates NR, Fatemi A. Fatigue life of 2024-T3 aluminum under variable amplitude multiaxial loadings: experimental results and predictions. *Procedia Eng*. 2015;101:159–168.

[14]Yao WX, Xia K, Gu Y. On the fatigue notch factor, K_f. *Int J Fatigue*. 1995; 17(4): 245–251.

[15]Taylor D. Geometrical effects in fatigue: a unifying theoretical model. *Int J Fatigue*. 1999;21(5): 413–420.

[16]Luo P, Yao WX, Susmel L, Li P. Prediction of fatigue damage region with the use of the notch critical plane approach for crack initiation and propagation. *Int J Fatigue*. 2020;135:105533.

[17]El Haddad MH. Dowling NE. Topper TH, Smith KN. J integral applications for short fatigue cracks at notches. *Int J Fract*. 1980;16(1):15–30.

[18]Susmel L, Lazzarin P. A bi-parametric Wöhler curve for high cycle multiaxial fatigue assessment. *Fatigue Fract Eng Mater Struct*. 2002; 25(1):63–78.

[19]Lazzarin P, Susmel L. A stress-based method to predict lifetime under multiaxial fatigue loadings. *Fatigue Fract Eng Mater Struct*. 2003; 26(12):1171–1187.

[20]Susmel L. Multiaxial fatigue limits and material sensitivity to non-zero mean stresses normal to the critical planes. *Fatigue Fract Eng Mater Struct*. 2008; 31 (3–4):295–309.

[21]Susmel L, Meneghetti G, Atzori B. A simple and efficient reformulation of the classical Manson–Coffin curve to predict lifetime under multiaxial fatigue loading—Part I: Plain materials. *J Eng Mater Tech*. 2009; 131(2).

[22]Wang Y, Susmel L. The Modified Manson–Coffin Curve Method to estimate fatigue lifetime under complex constant and variable amplitude multiaxial fatigue loading. *Int J Fatigue*. 2016; 83:135–149.

[23]Susmel L. A simple and efficient numerical algorithm to determine the orientation of the critical plane in multiaxial fatigue problems. *Int J Fatigue*. 2010; 32(11): 1875–1883.

[24]Susmel L, Taylor D. An elasto-plastic reformulation of the theory of critical distances to estimate lifetime of notched components failing in the low/medium-cycle fatigue regime. *J Eng Mater Tech*. 2010;132(2).

[25]Susmel L, Taylor D. Estimating lifetime of notched components subjected to variable amplitude fatigue loading according to the elastoplastic theory of critical distances. *J Eng Mater Tech*. 2015;137(1).

[26]Gates N, Fatemi A. Multiaxial variable amplitude fatigue life analysis including notch effects. *Int J Fatigue*. 2015;91:337–351.

[27]Wu ZR, Hu XT, Zhu L, Song YD, Li ZX. Evaluation of fatigue life for TC4 notched components under variable amplitude multiaxial loading. *Iran J Sci Technol Trans Mech Eng*. 2019;43(2):235–243.

[28]. Wu ZR, Hu XT, Li ZX, Song YD. Evaluation of fatigue life for titanium alloy TC4 under variable amplitude multiaxial loading. *Fatigue Fract Eng Mater Struct*. 2015; 38(4):402–409.

[29]Wu ZR,. Hu XT, Song YD. Multiaxial fatigue life prediction for titanium alloy TC4 under proportional and nonproportional loading. *Int J Fatigue*. 2014 59:170–175.

[30]Hertel O, Vormwald M. Short-crack-growth-based fatigue assessment of notched components under multiaxial variable amplitude loading. *Eng Fract Mech*. 2011;78(8):1614–1627.

[31]Tao ZQ, Shang DG, Sun YJ, Liu XD, Chen H, Li ZG. Multiaxial notch fatigue life prediction based on pseudo stress correction and finite element analysis under variable amplitude loading. *Fatigue Fract Eng Mater Struct*. 2018;41(8):1674–1690.

[32]Wang CH, Brown MW. A path-independent parameter for fatigue under proportional and non-proportional loading. *Fatigue Fract Eng Mater Struct*. 1993; 16(12):1285–1297.

[33]Wang CH, Brown MW. Life prediction techniques for variable amplitude multiaxial fatigue—part 1: theories. *J Eng Mater Tech*. 1996;118(3):367–370.

[34]Wang CH, Brown MW. Life prediction techniques for variable amplitude multiaxial fatigue—part 2: comparison with experimental results. *J Eng Mater Tech*. 1996; 118(3):371–374.

[35]Luo P, Yao WX, Susme L. An improved critical plane and cycle counting method to assess damage under variable amplitude multiaxial fatigue loading. *Fatigue Fract Eng Mater Struct*. 2020 (Published as early view). https://doi.org/10.1111/ffe.13281.

[36]Zhang CC, Yao WX. An improved multiaxial high-cycle fatigue criterion based on critical plane approach. *Fatigue Fract Eng Mater Struct*. 2010;34(5):337–344.

[37]Susmel L, Taylor D. A novel formulation of the theory of critical distances to estimate lifetime of notched components in the medium-cycle fatigue regime. *Fatigue Fract Eng Mater Struct*. 2007; 30(7):567–581.

[38]Bannantine JA, Socie DF. A variable amplitude multiaxial fatigue life prediction methods. ICBMFF3, 1990.

[39]Carpinteri A, Spagnoli A, Vantadori S. A multiaxial fatigue criterion for random loading. *Fatigue Fract Eng Mater Struct*. 2003; 26(6):515–522.

[40]Wu ZR. Research on multiaxial fatigue life prediction method for titanium alloy. In: Ph.D. Thesis. Nanjing: Nanjing University of Aeronautics and Astronautics; 2014 In chinese.

[41]Hoffmeyer J, Döring R, Seeger T, Vormwald M. Deformation behaviour, short crack growth

and fatigue livesunder multiaxial nonproportional loading. *Int J Fatigue*. 2006;28(5):508–520.

[42]Sonsino C. Fatigue testing under variable amplitude loading. *Int J Fatigue*. 2006; 29(6):1080–1089.

[43]Lagoda T, Sonsino CM. Comparison of different methods for presenting variable amplitude loading fatigue results. *Materialwissenschaft und Werkstofftechnik*. 2004; 35(1):13–20.

[44]Sonsino CM. Limitations in the use of RMS values and equivalent stresses in variable amplitude loading. *Int J Fatigue*. 1989;11(3):142–152.

Appendix 1 Dimensions and FE models of the notched specimens being investigated

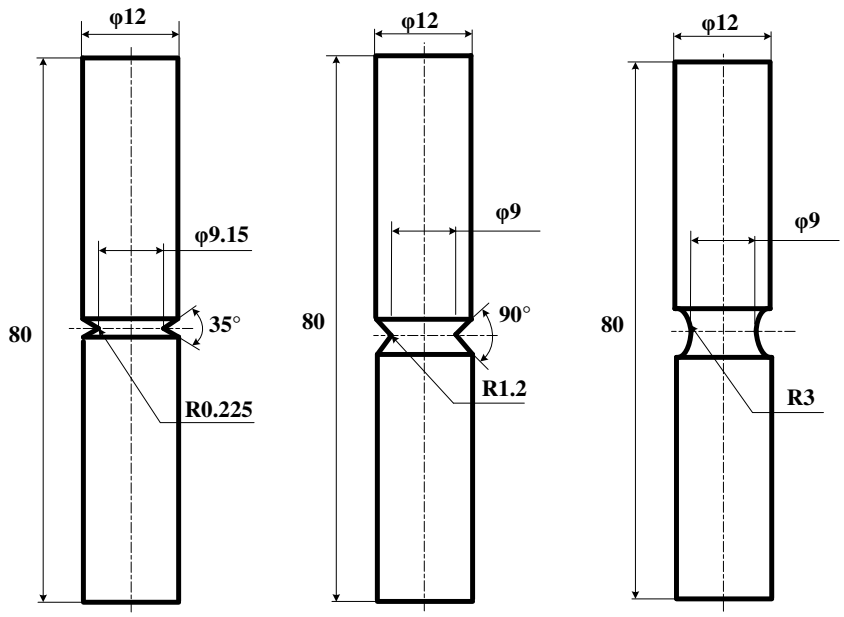

(*a*) The notched specimens made of C40

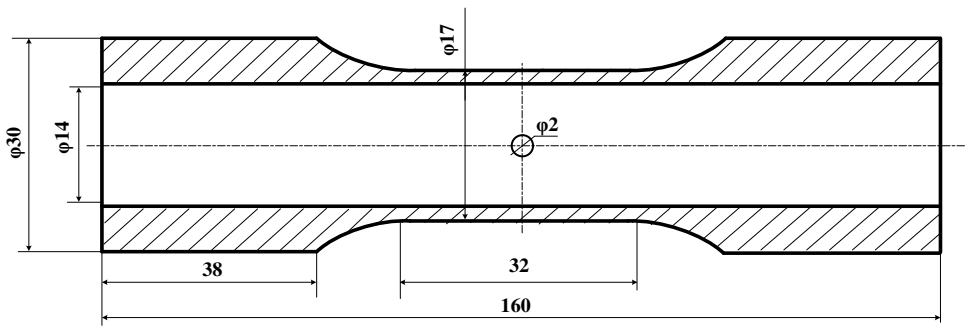

(*b*) The notched specimens made of TC4

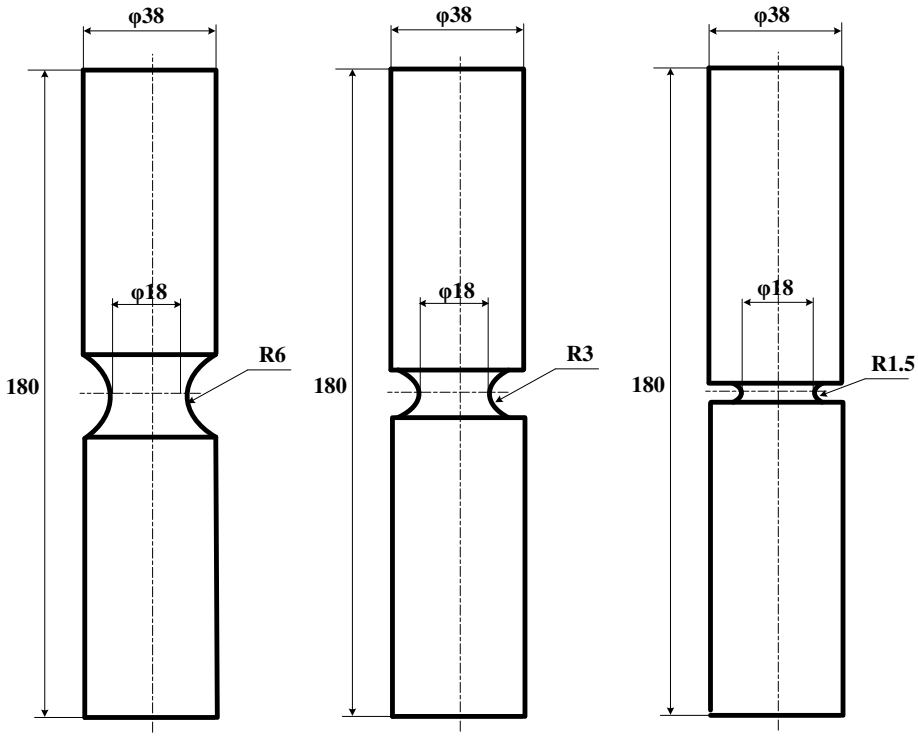

(*c*) The notched specimens made of En8

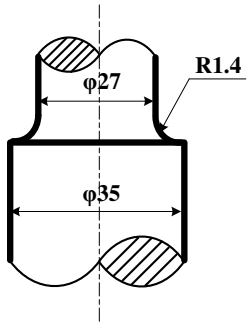

(*d*) The notched specimens made of S460N

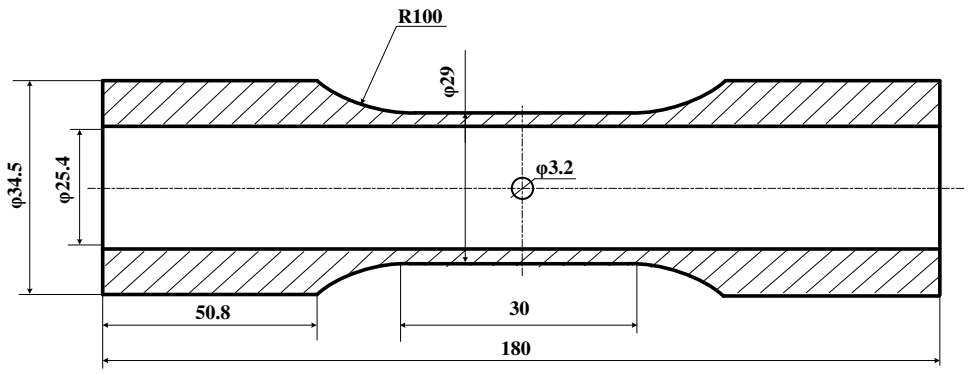

(*e*) The notched specimens made of 2024-T3

Figure A2.1 The dimensions of collected notched specimens

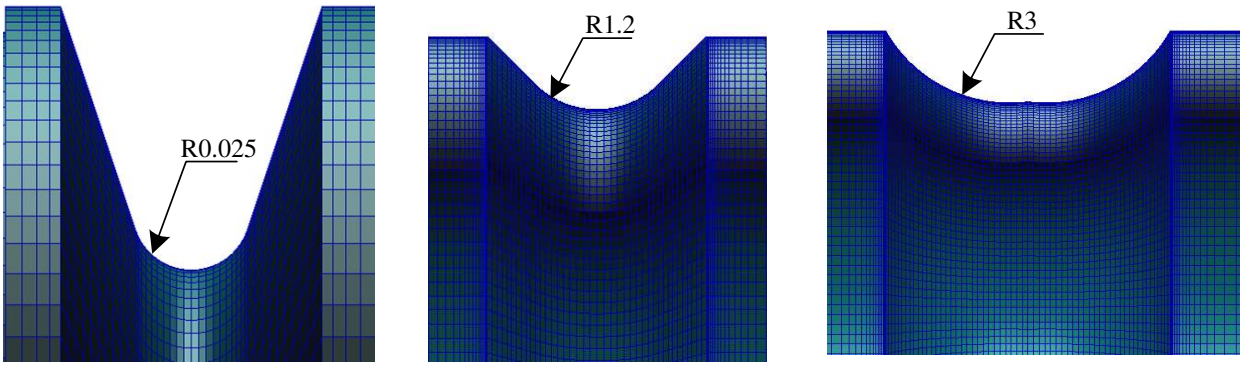

(*a*) The FE model of notched specimens made of C40

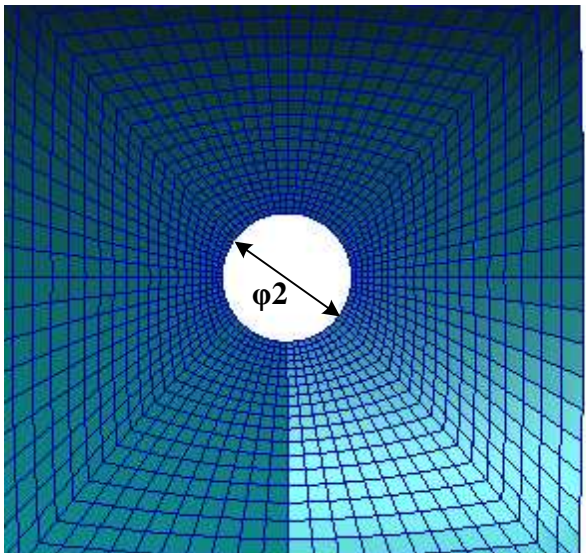

(*b*) The FE model of notched specimens made of TC4

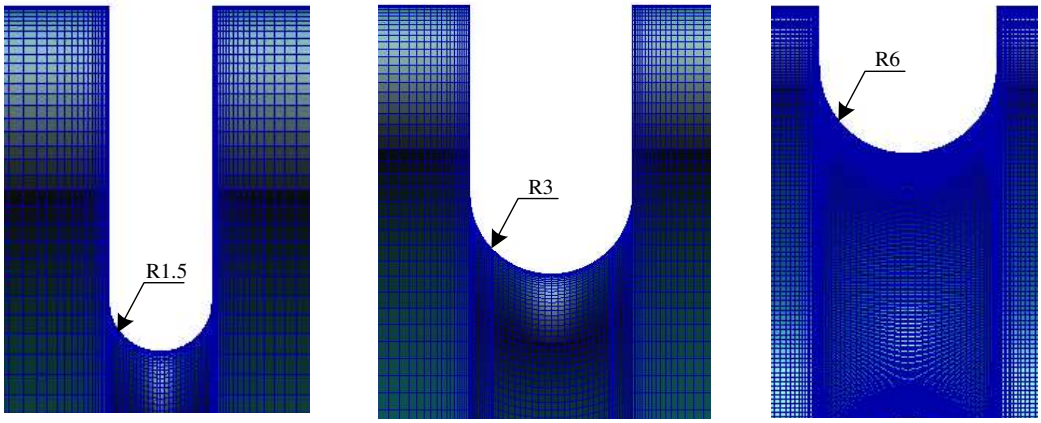

(*c*) The FE model of notched specimens made of En8

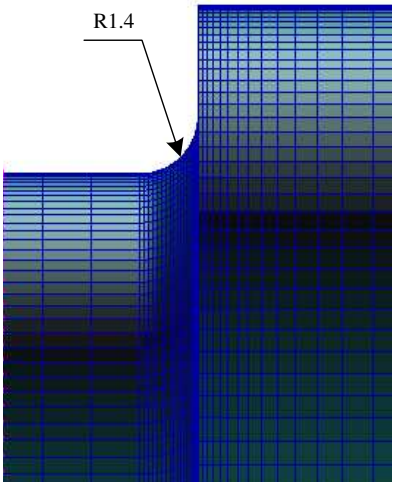

(*d*) The FE model of notched specimens made of S460N

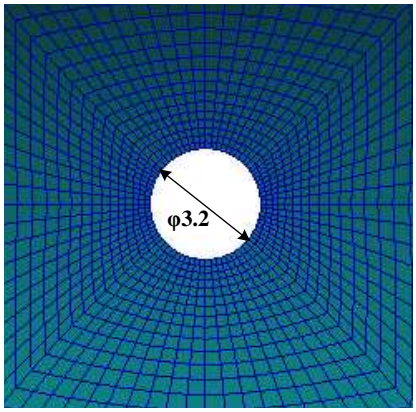

(*d*) The FE model of notched specimens made of 2024-T3

Figure A2.2 The FE models of collected notched specimens